Nonlinear 2D Convection and Enhanced Cross-Field Plasma Transport Near the MHD Instability Threshold.

V.P. Pastukhov, N.V. Chudin

RRC "Kurchatov Institute", 123182 Moscow, Russian Federation

e-mail: past@nfi.kiae.ru

Abstract. Results of theoretical study and computer simulations of nonlinear 2D convection induced by a convective MHD instability near its threshold in FRC-like non-paraxial magnetic confinement system are presented. An appropriate closed set of weakly nonideal reduced MHD equations is derived to describe the self-consistent plasma dynamics. It is shown that the convection forms nonlinear large scale stochastic vortices (convective cells), which tend to restore and to maintain the marginally stable pressure profile and result in an essentially nonlocal enhanced heat transport. A large amount of data on the structure of the nascent convective flows is obtained and analyzed. The computer simulations of long time plasma evolutions demonstrate such features of the resulting anomalous transport as profile consistency, L-H transition, external transport barrier, pinch of impurities, etc.

1. Introduction.

Anomalous plasma transport is one of the most intriguing problem of the magnetic plasma confinement for fusion. As a rule it is associated with fluctuations of plasma temperature and density caused by different kinds of drift wave instabilities. Due to small cross-field scales of the fluctuations the anomalous transport is conventionally discussed in terms of local transport coefficients. Considering a relatively simple magnetic field configuration as an example we demonstrate that in some cases the anomalous plasma transport could have another physical nature.

Here we present results of theoretical study and computer simulations of nonlinear 2D plasma convection which is induced and maintained by convective MHD instability near its threshold. The similar convection can appear in various plasma magnetic confinement systems, but it is especially typical for the plasmas confined in highly non-paraxial magnetic configurations with closed field lines, such as FRC [1, 2], LDX [3, 4] and some other high β alternative magnetic confinement systems (MIRAGE [5], EPSILON [6], etc.). Due to an unfavorable magnetic field-line curvature in the above systems it is typically expected [7, 8] that plasma pressure profiles have a tendency to be marginally stable with respect to flute-like interchange modes and, therefore, satisfy the condition: $S \equiv p\,U^{\gamma} = \text{const}$, where p is plasma pressure, $U = \oint dl/B$, γ is the adiabatic index, and S is a single-value function of entropy density of magnetized plasma. It is important to note that flute-like convective modes are marginally stable under the condition $S = \text{const}$ for any β values admitted by equilibrium conditions.

Contrary to the previous works we assume the marginally stable (MS) pressure profile as an initial condition only and describe the further plasma dynamics in the frame of weakly nonideal MHD equations with given plasma heating sources and original local thermal conductivity, viscosity, and resistivity. In this case the heating and the original thermal conductivity distort the initial pressure profile making it a weakly unstable. The instability induces and maintains a nonlinear MHD convection, which tends to restore the MS pressure profile and results in an essentially nonlocal, enhanced heat transport. As a first step we consider the self-consistent 2D convection and the corresponding plasma transport in a simple cylindrical quasi-equilibrium plasma column with a rigid current carrying rod of radius r_c at its axis. Such the model allows us to reproduce the most important features of plasma dynamics inherent in the magnetic confinement systems based on the levitated dipole (internal ring) [3, 4, 5] and in other FRC-like configurations with pure poloidal magnetic field. From the other hand side the cylindrical geometry appreciably simplifies calculations of high β plasma equilibria and their evolutions.

2. Basic Equations.

Very small ratio of typical ideal MHD times and dissipative times extremely complicates self-consistent computer simulations of the above plasma dynamics, especially, when we are interested in simulations of long time plasma evolutions at times of the order of plasma life-time. For fusion plasmas these time scales may differ by eight to nine orders of magnitude. To simplify the basic set of MHD equations we apply a variational method of adiabatic separation of fast and slow motions [9]. The method allows one to exclude from the consideration fast stable collective degrees of freedom without violating the conservation laws inherent in the basic (unreduced) set of equations. The last is very important for the correct description and simulations of the long time plasma evolutions.

The appropriate set of the adiabatically reduced weakly nonideal equations was derived in paper [10]. The derivation is based on the assumption (confirmed by further computations) that the self-consistent convection maintains the plasma pressure profile near the state which is marginally stable with respect to the flute-like interchange modes and deeply stable against all another ideal MHD modes. Typical plasma pressure profile in the internal ring (levitated dipole) systems is shown at FIG.1, where Ψ_c and Ψ_s correspond to the magnetic flux values at the internal conductor surface and at the external separatrix, respectively. The plasma is MHD stable in the inner region ($\Psi_c < \Psi < \Psi_m$) and marginally stable ($S(\Psi) = \text{const}$) in the outer region ($\Psi_m < \Psi < \Psi_s$). According to [10, 11, 12, 13], such pressure profiles are stable against all incompressible Alfvén perturbations (high n ballooning, large-scale kink ($m = 1;\ n = 1, 2$), etc), if β does not exceed some critical value $\beta_c \sim 1$. Assuming $\beta < \beta_c$, we can completely exclude the incompressible Alfvén perturbations. Therefore, in the simple cylindrical geometry, we analyze only flute-like 2D axisymmetric ($m = 0$) plasma motions.

As it was shown in [9, 10], the adiabatic separation principle allows us also to exclude compressional Alfvén (magnetosonic) degrees of freedom even in the high β case assuming that the dynamical plasma states under the consideration deviate only slightly from the MS state for the flute-like modes. For the weakly nonideal MHD the small parameter ϵ, which allows us to apply the adiabatic separation, has the form:

$$\epsilon \sim (\chi / a\, c_s)^{1/3} \ll 1 \ , \tag{1}$$

where χ is the original local thermal diffusivity, a is a minor radial scale, c_s is sound speed. The resulting adiabatic velocity field that completely describes the reduced plasma dynamics and does not perturb the fast stable degrees of freedom takes the form:

$$\mathbf{v}_a = \frac{1}{B^2}[\mathbf{B} \times \boldsymbol{\nabla}\Phi] \sim \epsilon\, c_s \ , \tag{2}$$

where an arbitrary function $\Phi(t, r, z)$ has the meaning of 2D electric potential.

The reduced equations are written in terms of more appropriate variables: the Jacobian of the transformation to flux coordinates $J = \mathbf{B} \cdot \boldsymbol{\nabla}\theta / 2\sqrt{\pi} = \sqrt{\pi}/U$, the entropy function $S = p/J^\gamma$, and the Lagrangian function of density $\lambda = \rho/J$ (introduced instead of B, p, and ρ, respectively), which allow us to account invariant features of the original MHD

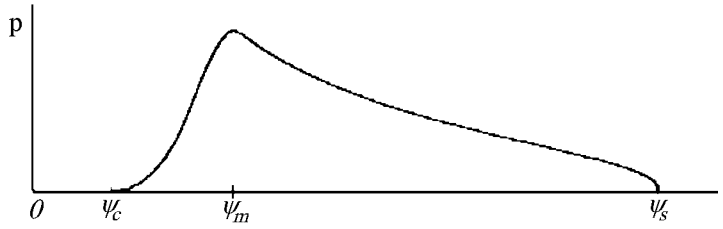

FIG. 1. Marginally stable plasma pressure profile in the levitated dipole.

equations explicitly. Assuming the closeness to the MS state, we represent the entropy function as $S(t,r,z) = \bar{S}(t,r) + \tilde{S}(t,r,z)$, where z-averaged quasi-equilibrium component $\bar{S}(t,r)$ satisfies the condition $\bar{S}'(r) > -\epsilon^2 \bar{S}/a$ and $\tilde{S} \sim \epsilon^2 \bar{S}$ describes fluctuations of the entropy function. Function λ admits the similar presentation. The reduced equations include a subset of coupled "fast" ($\partial/\partial t \sim \epsilon c_s/a$) equations, which describe 2D plasma dynamics and the entropy fluctuations $\tilde{S}$ and a subset of "slow" equations ($\partial/\partial t \sim \epsilon^3 c_s/a$), which describe 1D (radial) plasma transport in the presence of the convective motions and of the entropy fluctuations.

The reduced dynamical equation takes the form [10]:

$$\partial_t w + \frac{1}{r}\Big[\Phi,\ \frac{w}{J}\Big] + J^{\gamma-2}\frac{dJ}{rdr}\frac{\partial \tilde{S}}{\partial z} = \boldsymbol{\nabla}\cdot\left\{\frac{\boldsymbol{\nabla}(\bar{\eta}{C_A}^2 w)}{{C_A}^2}\right\}\ , \tag{3}$$

$$[\Phi,\ f] = \frac{\partial \Phi}{\partial z}\frac{\partial f}{\partial r} - \frac{\partial \Phi}{\partial r}\frac{\partial f}{\partial z}\ ,$$

where w is the contravariant component of the convective flow vorticity:

$$w = \boldsymbol{\nabla}\theta\cdot\left[\boldsymbol{\nabla}\times\left(\frac{\rho}{J}\mathbf{v}_a\right)\right] = \boldsymbol{\nabla}\cdot\left(\frac{\rho\boldsymbol{\nabla}\Phi}{r^2J^2}\right) = \boldsymbol{\nabla}\cdot\left(\frac{\boldsymbol{\nabla}\Phi}{{C_A}^2}\right)\ , \tag{4}$$

η is the local kinematic viscosity and C_A is the Alfvén speed. The equation for the entropy fluctuations has been derived in [10]. For this purpose the complete transport equation for the thermal plasma energy was rewritten in the terms of the new variables and its z-averaged component was eliminated:

$$\partial_t \tilde{S} + \frac{1}{rJ}\left[\Phi,\ \tilde{S}\right] - \frac{1}{rJ}\frac{d}{dr}\langle\tilde{S}\frac{\partial\Phi}{\partial z}\rangle + \frac{1}{rJ}\frac{\partial\Phi}{\partial z}\frac{d\bar{S}}{dr} \tag{5}$$

$$= \frac{\gamma-1}{2\gamma J^\gamma}\boldsymbol{\nabla}\cdot\left\{\bar{\rho}\bar{\chi}\left[c_s\boldsymbol{\nabla}\left(c_s\frac{\tilde{S}}{\bar{S}}\right) - c_s^5\boldsymbol{\nabla}\left(\frac{\tilde{\lambda}}{\bar{\lambda}\,c_s^3}\right)\right]\right\}\ ,$$

where the angular brackets denote averaging over z. The left-hand sides of Eqs. (3) and (5) describe the ideal plasma dynamics including the linear instability drive and the nonlinear mode coupling and saturation. In accordance with the assumed ordering, all the terms in these left-hand sides are of the same order of magnitude. The dissipative terms on the right-hand sides are as small as $\epsilon^2 a^2|\nabla_\perp|^2$ in comparison with the left-hand sides. The equation for $\tilde{\lambda}$ is similar to the equation for $\tilde{S}$.

The adiabatic velocity field (2) does not perturb the magnetic field. Therefore, there are no "fast" fluctuations of J, and the frozen-in equation with a small resistivity gives the first of the "slow" equations:

$$\partial_t J = \frac{1}{r}\frac{d}{dr}r\Big(-uJ + \frac{\bar{D}}{r^2}(r^2J)'\Big)\ , \tag{6}$$

where $D = c^2/4\pi\sigma$ is the local magnetic field diffusion coefficient and $u(\epsilon^3 t,\ r) \sim \epsilon^3 c_s$ is a slowly variable ("diffusive") radial velocity that has to be added to the adiabatic velocity (2) in the "slow" equations [10]. The second "slow" equation corresponds to the main radial forces balance (quasi-equilibrium):

$$J\frac{d}{dr}\Big(\frac{\gamma\bar{S}}{\gamma-1}J^{\gamma-1} + r^2J\Big) - \frac{J^\gamma}{\gamma-1}\frac{d\bar{S}}{dr} = 0\,. \tag{7}$$

Eq. (7) determines $J(t,r)$ through the known $\bar{S}(t,r)$, while Eq. (6) serves to determine u. Equation for $\bar{S}$ is the z-averaged component of the complete heat transport equation:

$$\partial_t \bar{S} + u\,\frac{d\bar{S}}{dr} + \frac{1}{rJ}\,\frac{d}{dr}\langle \tilde{S}\,\frac{\partial \Phi}{\partial z}\rangle = \frac{\gamma-1}{J^\gamma}\,\bar{Q}_E \tag{8}$$

$$+\frac{\gamma-1}{2J^\gamma}\,\frac{1}{r}\,\frac{d}{dr} r\left\{\bar{\lambda} J \bar{\chi}\,\frac{d}{dr}\left(\frac{J^{\gamma-1}\,\bar{S}}{\bar{\lambda}}\right)\right\} - \frac{\gamma \bar{S}}{rJ}\,\frac{d}{dr}\left\{\frac{\bar{D}}{r}(r^2 J)'\right\}\ ,$$

where $\bar{Q}_E(r,\,t)$ describes an energy source. All the terms in Eq. (8) are of the order of ϵ^3. The third term in the left-hand side of Eq. (8) describes the nonlocal heat transport caused by 2D convection. The equation for $\bar{\lambda}$ is similar to the equation for $\bar{S}$.

3. Formulation of the Evolutionary Problem.

The self-consistent plasma convection and the convective enhancement of transport processes were simulated as an evolutionary problem with given initial and boundary conditions in the frame of equations presented in the Sec. 2. It is assumed that the plasma occupies the region between the central conductor of radius r_c and the external magnetic surface of radius r_s, which plays the role of a poloidal separatrix. All of the functions are assumed to be periodic in z (the period being $2\pi R$) and are described by the "toroidal" angle $\varphi = z/R$. The initial profile of $\bar{S}$ was chosen in the form: the function $\bar{S}$ increases monotonically from $\bar{S} = S_c \ll S_m$ to $\bar{S} = S_m$ at the interval $r_c \le r \le r_m$, and $\bar{S} = S_m =$ const at the interval $r_m \le r < r_s$. The initial perturbations are taken as follows: $\Phi|_{t=0} = 0$, while $\tilde{S}(0,r,\varphi)$ is a sufficiently small arbitrary function ($|\tilde{S}|_{t=0} \ll \epsilon^2 S_m$). The energy source $Q_E(r)$ has a parabolic profile centered at the surface $r = r_m$. All quasi-steady functions and parameters are normalized to the dimensionless form by their initial values at the surface $r = r_m$: $x = r/r_m$, $s_0(x,t) = \bar{S}/S_m$, etc. Specifying $\epsilon = (\chi_m/2r_m c_s)^{1/3}$, we introduce the dimensionless time $\tau = \epsilon c_s t/r_m$ and normalize the fluctuating functions according to their ϵ-ordering: $\tilde{s} = \tilde{S}/\epsilon^2 S_m$, etc. (see [10] for details).

The Jacobian J at the inner plasma boundary is determined by the current I_c in the central conductor: $J(r_c) = J_c = I_c/\sqrt{\pi} c r_c^2$. The dimensionless Jacobian is defined as $g = J/J_c x_c^2$. The function s_0 is fixed at the conductor surface. At the external boundary:

$$\partial_x s_0(x_s,\tau) \;=\; -\nu s_0(x_s,\tau)\ . \tag{9}$$

The last condition allows us to model the enhanced energy losses near the separatrix by choosing sufficiently large values of ν. Since both the conductor surface and the separatrix (due to the presence of magnetic null points) have to be equipotential surfaces, the boundary conditions for the φ-dependent component of the potential $\tilde{\phi} = \phi - \phi_0(x,\tau)$ have the form $\tilde{\phi}(x_c,\varphi,\tau) = \tilde{\phi}(x_s,\varphi,\tau) = 0$. The similar boundary conditions can be imposed on the entropy fluctuations: $\tilde{s}(x_c,\varphi,\tau) = \tilde{s}(x_s,\varphi,\tau) = 0$. The averaged component of the potential $\phi_0(x,\tau)$ describes zonal flows which are linearly stable and are generated due to the nonlinear mode coupling. We assume that the zonal flow velocity vanishes at the central conductor: $\partial_x \phi_0(x_c,\tau) = 0$. Following the paper [10], we also impose the condition of zero vorticity flux density at both the boundaries.

Function $\tilde{\lambda}$ (contrary to $\tilde{S}$) does not play a decisive role in the sustenance of the self-consistent plasma convection and in the formation of the MS pressure profiles. Therefore, following [10], we self-consistently exclude the plasma density transport from the consideration for a simplicity. For this purpose we assume that D and density source Q_ρ are equal to zero, along with $\bar{\lambda}(t,r) =$ const and $\tilde{\lambda}(t,r,\varphi) = 0$. So that we need not to solve the corresponding equations. Below we illustrate the ability of the convective flows to form

and to maintain the profile $\bar{\lambda}(t,r) \approx$ const considering an evolution of "passive impurity" density ρ_* which does not influence the main plasma dynamics and is only stirred by the self-consistent plasma velocity field.

4. Results of the Computer Simulations.

The reduced set of equations for $\tilde{s}$, w, ϕ, s_0, and g with the above boundary and initial conditions was solved at the radial interval $x_c = 0.5 \leq x \leq x_s = 2$. All calculations were carried out for the fixed parameter $\epsilon = 0.1$, while the other parameters were varied. The total computation time τ_{tot} was chosen to be greater than the plasma energy lifetime and was varied from 50 to 450 for different shots. The results of simulations carried out with $\beta_{max} = 0.5$, aspect ratio $A = R/r_m = 2$, and $\nu = 2 \div 4$ are illustrated in FIGs. 2–6. The initial linear and quasilinear stages of MHD instability last about $\tau = 5$. Then the convective flows and the entropy fluctuations come to a stage of highly nonlinear rearrangement. This stage is highly irregular and leads to formation of broad frequency and wave-number spectra. After $\tau \approx 20$ the plasma comes to a stage of quasisteady turbulence, at which the profile of s_0 as well as the spectrum width remain almost unchanged. The convective flows acquire a certain characteristic large-scale vortex structures while remaining at a fairly high level of stochasticity.

Typical two-dimensional structures of convective flows and of entropy fluctuations at the quasisteady stage (at $\tau = 40.7$) is shown at FIG. 2. FIG. 2a shows the contours of $\phi =$ const, or, equivalently, the streamlines of the flows. The light and dark regions correspond to the positive and negative values of the potential, respectively. The flow structures are dominated by one or two long-lived pairs of coupled large-scale vortices with the strictly definite polarity. The vortices are localized almost completely in the region $1 < x < 2$, where $s_0' \approx 0$, and evolve in a fairly complicated and irregular manner, changing their intensity and shape and drifting along φ. The characteristic feature of these vortex pairs is the presence of a fairly fast plasma jets localized in the ϕ coordinate ($\varphi \approx 2.1$ and $\varphi \approx 4.4$ at FIG. 2a) and directed from the separatrix to the plasma center. FIG. 2b shows levels of the entropy fluctuations $\tilde{s}$. The entropy fluctuations have smaller spacial scales and are more stochastic in comparison with the plasma flows. FIG. 2c showes an early stage of fast penetration of the "passive impurity" mentioned in Sec. 3.

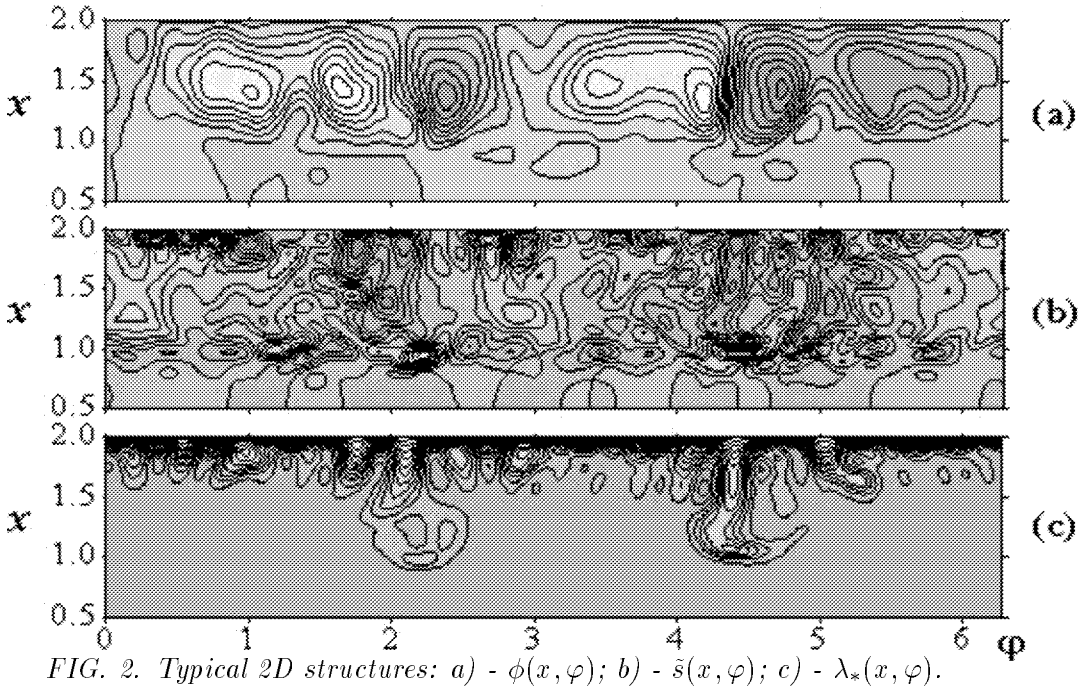

FIG. 2. Typical 2D structures: a) - $\phi(x,\varphi)$; b) - $\tilde{s}(x,\varphi)$; c) - $\lambda_*(x,\varphi)$.

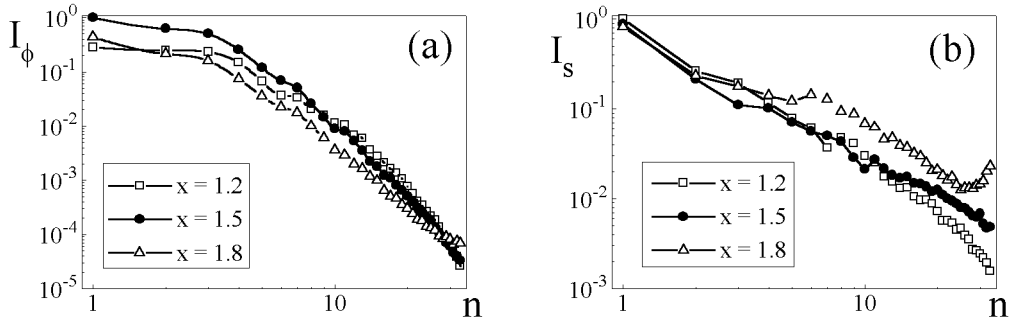

FIG. 3. Toroidal wave-number spectra of fluctuations: a) potential; b) entropy.

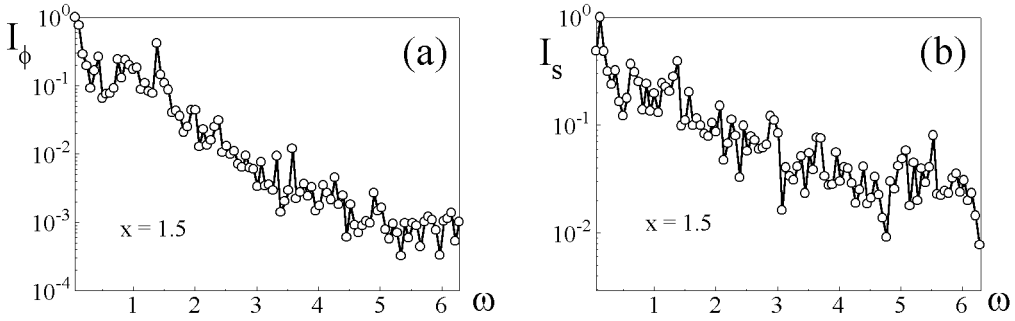

FIG. 4. Dimensionless frequency spectra of fluctuations: a) potential; b) entropy.

Lagrangian function of the impurity density $\lambda_* = \rho_*/J$ was "switched on" near the separatrix ($x = x_s$) at $\tau = 40$. One can see that the jets result in the fast injection of the impurity to the plasma core. Later in time, as it is shown at FIG. 5b, the convective flows form a plateau $\bar{\lambda}_*(x,\tau) \approx$ const which is similar to the MS plateau for $\bar{S}(x,\tau)$ and is consistent with the assumption $\bar{\lambda} =$ const that we have used for the main plasma density.

FIG. 3 displays the time-averaged spectra of the potential and of the entropy fluctuations computed as functions of the toroidal wave number n at three radial positions. One can see that the spectrum of the potential fluctuations I_ϕ (FIG. 3a) is dominated by toroidal harmonics with the numbers 1, 2, and 3. For higher harmonics the spectrum $I_\phi \propto n^{-4}$ and decreases even more sharply for $n > 12$ due to the dissipation of small-scale fluctuations. The spectrum of the entropy fluctuations (FIG. 3b) decreases approximately as $I_s \propto n^{-1.5}$ at the inertial interval $1 \leq n < 12$. At an arbitrary instant of time, the n-spectra of the fluctuations can differ substantially from the time-averaged spectra shown at the FIG. 3.

FIG. 4 displays the dimensionless frequency spectra. The potential spectrum $I_\phi(\omega)$ (FIG. 4a) has a dominant low-frequency part ($\omega < 1.5$) and decreases on the average as $\omega^{-3.6}$ at higher frequencies. It also exhibits a set of minor peaks which follow with an interval $\Delta\omega \approx 0.46$. The spectrum of the entropy fluctuations $I_s(\omega)$ (FIG. 4b) is wider and less regular than $I_\phi(\omega)$.

FIG. 5 shows radial profiles of quasisteady parameters at the stage of fairly well developed turbulence ($\tau = 100$). As it has been expected, the profile $s_0(x,\tau)$ (solid curve at FIG. 5a) has a plateau in the region of 2D convection $1 < x < 2$. The maintenance of the plateau (deviations from $s_0 =$ const are smaller than 3%) was observed over all time intervals including transition regimes. The last means the consistency of pressure and temperature profiles in the convective region. For a fixed energy source the steady state level of s_0 in the plateau region and the corresponding plasma life-time depend only on ν-value.

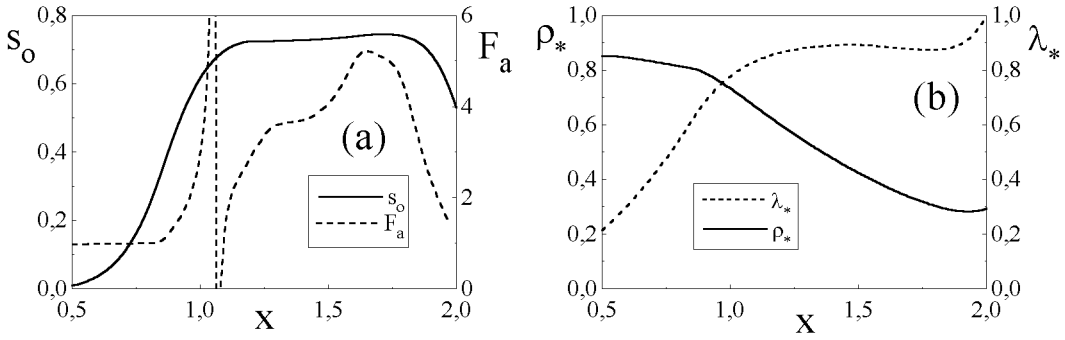

FIG. 5. Radial profiles: a) entropy and anomaly factor; b) averaged impurity density.

Following the traditional interpretation of experimental data on anomalous transport we formally introduce the effective (anomalous) local thermal diffusivity $\chi_{eff} = -\bar{q}/\rho\bar{T}'$, where $\bar{q}(x,\tau)$ and $\bar{T}(x,\tau)$ are the calculated values of thermal flux density and temperature. For convenience, we also introduce an "anomaly factor", which is defined as the ratio of the effective thermal diffusivity to the classical one: $F_a = \chi_{eff}/\chi_{cl}$. The anomaly factor is shown by the dashed curve at FIG. 5a. $F_a \approx 1$ in the region $0.5 < x < 0.9$ that indicates that the heat transport is classical one there. Alternating-sign spikes near the magnetic surface $x = 1.1$ correspond to the fact that $\bar{q}(x,\tau)$ and $\bar{T}'(x,\tau)$ vanish at different magnetic surfaces. In the convective region at larger radii, the factor F_a first increases to its maximum value (which depends on ν) and then, near the plasma boundary, drops down to the unity. The steep decrease of F_a near the plasma edge is entirely consistent with the notion of an "external transport barrier". FIG. 5b illustrates the radial distribution of the "passive impurity" density. The dashed curve presents the φ-averaged Lagrangian function $\bar{\lambda}_*(x)$ which, analogously to $\bar{s}(x)$, has a plateau in the convective region. The corresponding profile of the impurity density $\rho_*(x)$ increases towards the plasma core. One can interpret the formation of such the profile as a "pinch of impurities". From the other hand side the fast penetration of impurities can be considered as an effective mechanism for the core plasma fueling from the periphery.

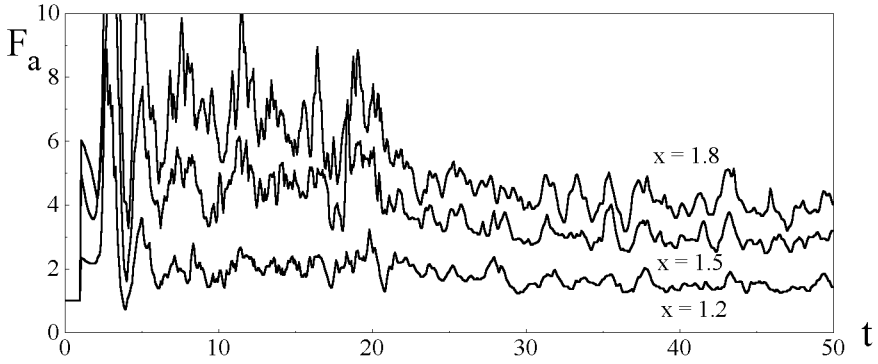

FIG. 6. Evolution of the anomaly factor at three radial positions.

FIG. 6 presents the time evolution of the "anomaly factor" F_a at three radial positions in a shot in which the energy absorption at the plasma edge quickly changes at a particular moment of time, i.e. factor ν in the boundary condition (9) decreases from 4 to 2 at $\tau = 20$. The figure shows that the anomaly factor F_a decreases appreciably over all the region of the convection during a short interval about 4-5 characteristic times while the relative temperature gradients in the main plasma volume are still unchanged. Such the behavior of the effective transport coefficients is similar to L-H transitions in tokamaks.

5. Conclusion.

The theoretical analysis and computer simulations of the nonlinear 2D convection, which develops self-consistently near the threshold for the ideal MHD instability, are presented. The convection is generated and maintained by the competition of two processes: the plasma heating and local dissipative processes distort the initial MS plasma pressure profile giving rise of weakly unstable perturbations, which then restore the MS profile and result in the essentially nonlocal enhanced heat transport. The adiabatically reduced equations provide the self-consistent description of relatively fast nonlinear convective flows and of slower transport processes in weakly dissipative high β plasmas. The equations derived in such the manner conserve the invariant properties of the basic ideal MHD equations and, therefore, they can be used to simulate the plasma evolutions at arbitrary long time intervals (longer than the plasma lifetime).

The computer simulations have shown that the convection at the stage of fairly well developed turbulence is essentially nonlinear and has wide frequency and wave-number spectra. A finite number of large-scale long-living stochastic vortices (convective cells) dominates in the 2D flow structures. The convection maintains a quasisteady turbulent-relaxed plasma state, which is characterized by the MS plateau in the radial profile of the entropy density as well as by the plateaus in the profiles of Lagrangian functions of densities of plasma components. The maintenance of the plateaus could be interpreted as the "profile consistency" and as the "pinch of impurities" in the convective region. The convection results in the enhanced heat transport whose rate is determined by the energy losses at the plasma periphery rather than by the relative gradients of plasma parameters in the main confinement region. This effect looks as L-H transitions in tokamaks. The steep decrease of the conventionally defined anomalous thermal diffusivity could be interpreted as an "external transport barrier". The results obtained are important not only for the magnetic confinement systems with internal levitated conductors (like those modeled in the paper) but also for other systems with plasma pressure profiles which are marginally stable against ideal MHD modes.

Acknowledgments. The work was supported in part by the Council of the Federal Program "Government Support of the Leading Scientific Schools", project 00-15-96526.

References

[1] ES'KOV A.G., KURTMULLAEV R.Kh., et al., Proc. 7th Int. Conf. on Plasma Phys. and Cont. Nucl. Fusion Res., Innsbruck, 1978. Nucl. Fusion Suppl., IAEA, Vienna (1979), Vol.2, p. 187.
[2] ARMSTRONG W.T., LINFORD R.K., et al., Phys. Fluids, **24**, (1981) 2068.
[3] HASEGAVA A., CHEN L., and MAUEL M.E., Nucl. Fusion, **30**, (1990) 2405.
[4] KESNER J., BROMBERG L., GARNIER D.T., and MAUEL M.E., Fusion Energy 1998 (Proc. 17th Int. Conf. Yokohama, 1998), IAEA, Vienna (1999), Vol.3, p. 1165.
[5] MOROZOV A.I., PASTUKHOV V.P., and SOKOLOV A.Yu., Proc. of Workshop on D-3He Based Reactor Studies, Moscow, 1991 (Kurchatov Inst. of Atomic Energy, Moscow, 1991), p. 1C1.
[6] ARSENIN V.V., DLOUGACH E.D., et al., Nucl. Fusion, **41**, (2001) 945.
[7] VABISHCHEVICH P.N., DEGTYAREV L.M., DROZDOV V.V., et al., Sov. J. Plasma Phys., **7**, (1981) 536.
[8] POPOVICH P.A. and SHAFRANOV V.D., Plasma Phys. Reports, **26**, (2000) 484.
[9] PASTUKHOV V.P., ibid., **26**, (2000) 529.
[10] PASTUKHOV V.P. and CHUDIN N.V., ibid., **27**, (2001) 907.
[11] KRASHENINNIKOV S., CATTO P., and HAZELTINE R.D., Phys. Rev. Lett., **99**, (1999) 2689.
[12] GARNIER D.T., KESNER J., and MAUEL M.E., Phys. Plasmas, **6**, (1999) 3431.
[13] SIMAKOV A.V., CATTO P., KRASHENINNIKOV S., et al., ibid., **7**, (2000) 2526.